

Article

Post-Fire Mechanical Degradation of Lightweight Concretes and Maintenance Strategies with Steel Fibers and Nano-Silica

Alaa Fahad Mashshay, S. Komeil Hashemi *  and Hamidreza Tavakoli 

Civil and Structural Engineering, Civil and Environmental Engineering School, Babol Noshirvani University of Technology, Babol 4714873113, Iran; alaaafah87@gmail.com (A.F.M.); tavakoli@nit.ac.ir (H.T.)

* Correspondence: k.hashemi@nit.ac.ir

Abstract: Currently, the growth of building construction and the need for lighter but more sustainable materials are of interest. Additionally, recent fire incidents highlight the insufficient knowledge of the properties of materials after a fire. Common materials such as concrete should, to minimize their adverse environmental effects and expenses, be maintained in such a way as to increase their resistance and preserve their mechanical properties when subjected to high temperatures. Hence, in this research, the post-fire mechanical degradation of lightweight concrete (LWC) has been investigated. Moreover, the addition of steel fiber and nano-silica have been studied in terms of their ability to reduce the mechanical degradation of LWC subjected to high temperatures. For this purpose, different samples were considered in four mixture designs: the LWC samples, samples with steel fibers, samples with nano-silica, and samples with a combination of steel fibers and nano-silica. All samples were subjected to temperatures of 200, 400 and 600 degrees Celsius and compared with the control samples. The results show that, as the temperature increased, the tensile and compressive resistances of LWC decreased. The samples without fibers and nano-silica showed a greater decrease in mechanical properties with increasing temperature. The addition of steel fibers and nano-silica, individually or as a combination, can improve the compressive and tensile strength of the concrete both at room temperature and at higher temperatures.

Keywords: lightweight concrete; LECA; nano-SiO₂; steel fiber; post fire; sustainable materials



Citation: Mashshay, A.F.; Hashemi, S.K.; Tavakoli, H. Post-Fire Mechanical Degradation of Lightweight Concretes and Maintenance Strategies with Steel Fibers and Nano-Silica. *Sustainability* **2023**, *15*, 7463. <https://doi.org/10.3390/su15097463>

Academic Editor:
Constantin Chaliors

Received: 20 February 2023
Revised: 26 April 2023
Accepted: 28 April 2023
Published: 1 May 2023



Copyright: © 2023 by the authors. Licensee MDPI, Basel, Switzerland. This article is an open access article distributed under the terms and conditions of the Creative Commons Attribution (CC BY) license (<https://creativecommons.org/licenses/by/4.0/>).

1. Introduction

Currently, the growth of building construction and the need for lighter but more sustainable materials are of interest. Lightweight concrete (LWC) is a type of concrete with a specific weight—lower than 1920 kg/m³—and which is used frequently in construction projects as structural and non-structural building materials. Different types of LWC have been widely investigated and successfully developed and utilized in recent years to satisfy the need for lighter materials [1]. Moreover, one of the major issues in earthquake-proof structure design, especially for tall buildings and long bridges made of concrete, is the self-weight of the material. Hence, LWC with good mechanical properties (such as compressive and tensile strength) provides advantages that include a reduction in the dead load and, as a result, the seismic force. This leads to a more economical design and less seismic damage and, subsequently, more sustainable construction material. Since the strength of concrete is often directly related to its specific weight, the use of LWC by itself is not recommended due to the possible degradation in its mechanical properties.

Additionally, recent fire incidents in buildings have highlighted the insufficient knowledge of the properties of post-fire materials. Therefore, there is a growing need for approaches to post-fire maintenance for both construction materials and structural elements in order to enhance their fire safety [2–4]. Common materials such as concrete should be maintained in such a way that, after exposure to high temperatures, they offer more resistance and preserve more of their mechanical properties so as to achieve benefits both

in terms of minimizing their carbon footprint and in terms of the overutilization of natural resources. Hence, it is necessary for the materials used in structures to be sufficiently fire-proof [5]. Heat reduces the weight and compressive strength of concrete samples [6]. In extreme cases, post-fire concrete structures which are not prepared to withstand high temperatures no longer have the capacity to provide even serviceable limit states. Concrete maintains its structure up to a temperature of 200 °C, beyond which it begins to lose its physical properties. Furthermore, a rise in temperature leads to a strong decrease in the tensile properties of the concrete, a reduction in the rebar–concrete adhesion, the elimination of hydration, and, as a result, a large increase in the volumetric water absorption capacity [7,8].

Accordingly, improving the strength of LWC by adding certain materials may be a suitable option for various structural components in order to decrease their structural weight, and the earthquake damage they might receive, while securing their functionality. Though LWC is more expensive than normal concrete, when structural weight is taken into account in the design process the resulting buildings cost less when they are built with LWC than when they are built with normal concrete [9].

There are various methods for enhancing LWC. Fiber reinforcement in concrete will significantly increase the compressive strength, ductility, toughness and energy absorption. Fibers are categorized as metallic, polymeric compound, or natural. Among these, steel fibers are among the additives that are commonly used for many structural and non-structural functions. Researchers have reported different concrete properties while using steel fibers. Many have found that adding steel fiber to LWC by up to 1.5% by volume increases the compressive strength from 5 to 25% [10–14]. Some studies have shown that steel fiber has no significant influence on the compressive strength of LWC or have reported an efficient volume fraction of steel fiber to achieve the largest strength [15–18]. The effectiveness of steel fiber on the post-fire properties of steel-fiber-reinforced LWC (SFRLWC) has been examined by Wang et al. [8]. According to their results, an increase in the temperature reduced both the axial compressive strength and the modulus of elasticity while increasing the peak axial strain. Moreover, the stress–strain curves gradually flattened out. In addition, the toughness of all of the concrete samples first increased, then decreased due to a rise in the temperature. The addition of steel fibers can enhance the energy absorption capacity, toughness, and residual tensile strength of LWC before and after exposure to high temperatures. Huang et al. [19] investigated the simultaneous effect of temperature and strain rate on the mechanical properties of steel-fiber-reinforced concrete (SFRC). Their results indicate that SFRC exhibits a strain-rate-hardening effect. Kalpana et al. [20] reviewed the papers addressing SFRLWC. They state that steel fibers can reduce the brittleness of concrete and improve its ductility; however, the amount of change in LWC properties is reliant on the steel fiber’s volumetric percentage. Because both mechanical properties and fire protection are of interest in this research, the use of steel fiber itself cannot provide enough enhancement to concrete and some other additions are required.

When discussing the effects of high temperature on concrete, it is well known that one of the reasons behind the deterioration of a concrete’s properties is the decomposition of cement hydrate, yielding calcium oxide. Hence, by improving the constituent compounds in the concrete paste, it is possible to improve the strength of LWC when it is subjected to fire. For this reason, the addition of fine particles to mixture design was found to be very effective for the improvement of strength, flexibility, and durability in concrete. Among these, nano-silica (nano-SiO₂) can be an excellent substitute for traditional cement in LWC and will cause high fluidity levels, making the microstructure denser and more homogenous.

Balapour et al. [21] reviewed papers addressing the effects of nano-silica on the mechanical properties, ductility, durability, and microstructural properties of concrete. According to the authors, the long-term durability of concrete has been of interest to researchers in recent decades, and they have attempted to improve this parameter by various methods. A common technique used for this purpose is the addition of a new

material to concrete. One material that has attracted researchers' attention in this area is nano-SiO₂. Nano-silica can elevate cement hydration and reacts with free lime which leads to the formation of a great amount of C-S-H gel and, as a result, a densification of the cement matrix. Furthermore, nano-silica can fill the micro-pores in the microstructure and in the interfacial transition zone (ITZ) and reduce porosity.

Nazari and Riahi [22] investigated the effect of zero to 5% Nano-SiO₂ replacement on the compressive strength, flexural strength, thermal properties and microstructure of self-compacting concrete with w/b ratio of 0.4. Their investigation revealed that an addition of nano-silica up to 4% led to an increase in compressive strength, while an increase in replacement level led to its reduction. A similar trend in the improvement of the compressive and flexural strengths of concrete via the incorporation of nano-silica particles has also been reported by other researchers [23–25]. Furthermore, Wang et al. [26] performed an empirical study of the impact of nano-silica on the compressive strength, shrinkage, and initial crack sensitivity of lightweight aggregate concrete (LWAC).

In addition, Tobbala et al. [27] studied the mechanical properties of different high strength concrete mixes incorporated with nano-silica and nano-ferrite subjected to high temperatures of up to 800 °C. The specimens were assessed via scanning electron microscopy, compression and splitting tensile tests. Their results show that the compressive strength of the heated specimens with 3% nano-silica was better than those with 2% nano-ferrite at temperatures of 200–800 °C. With regard to the microstructure feature, their results confirm that nano-silica acted as an adequate filling material; one which produced a condensed microstructure with extra compressed hydration outputs.

Given the various advantages of LWC, it can be of great help in construction. Its only disadvantages are its low tensile and compressive strengths and its unknown behavior in cases of fire. Accordingly, in this research, the post-fire mechanical degradation of LWC has been investigated. Moreover, for the purposes of reducing the mechanical degradation of LWC subjected to high temperatures, the addition of steel fiber and nano-silica have been studied. For this purpose, different samples were casted in four mixture designs; LWC samples; samples with steel fibers up to 1, 1.5 and 2% volumetric fractions of LWC; samples with nano-silica of up to 1, 3 and 5% of the cement's weight; and a fourth mixture containing samples with a combination of 1% steel fibers and 3% nano-silica. All samples were subjected to temperatures of 200, 400 and 600 degrees Celsius and were compared with the control samples at room temperature. To do this, the axial compressive strength, tensile splitting strength and axial stress–strain curves tests, as well as the behaviors of the modulus of elasticity of the different samples at various temperatures, were studied.

2. Experimental Test and Methods

2.1. Raw Material Specifications

The materials employed for preparing the samples are reported in this section. Lightweight expanded clay aggregate (LECA) coarse grain with a maximum grain size of 12 mm, produced by the Leca Provider Company [28] was employed as lightweight coarse aggregate. A view of the LECA coarse grain can be seen in Figure 1. Crushed SiO₂-based continuous graded fine aggregates with a maximum dimension of 4.75 mm was used as sand. The sieve analysis test was performed according to ASTM C330 [29] and ASTM C33 [30] for LECA and sand, respectively. Results are presented in Figure 2. In addition, the mechanical and physical properties of LECA are tabulated in Table 1.

Table 1. Mechanical and physical properties of the LECA coarse aggregate.

Material Type	Maximum Size mm	Density (Compact) kg/m ³	Density (Loose) kg/m ³	Water Absorption %
LECA	12	700	650	6.9
Sand	4.75	2630	-	1.3



Figure 1. LECA coarse grain used in this research as gravel.

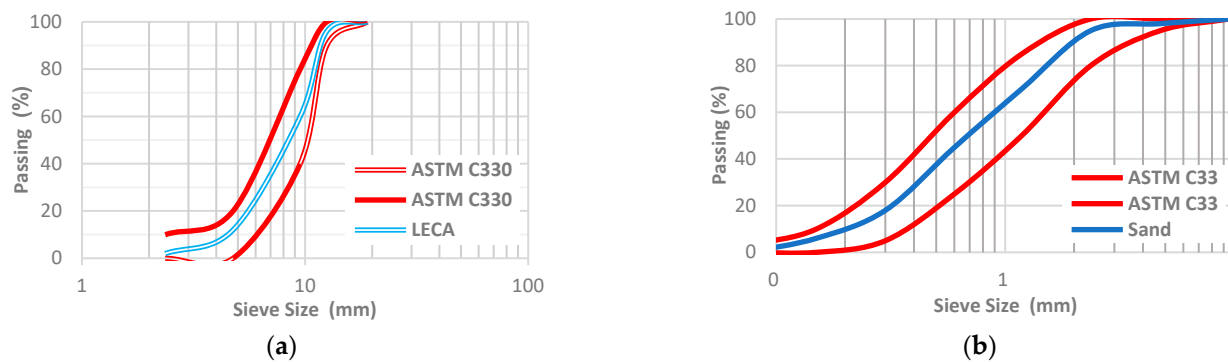


Figure 2. Sieve analysis. (a) Coarse aggregate (LECA); (b) fine aggregate (sand).

Portland cement type 2 was used in all samples. In addition, to achieve a sufficient slump in samples, a third-generation carboxylate-based, green-colored superplasticizer, trademarked as P8-3R, was used in a proportion of 2% of the cement's weight. The superplasticizer had a specific weight of 1050 kg/m^3 . The nano-silica used in this research was in the form of a white powder with a particle size of 11–13 nm and a purity of 99%. The TEM and XRD images of this material are shown in Figure 3 and Figure 4, respectively.

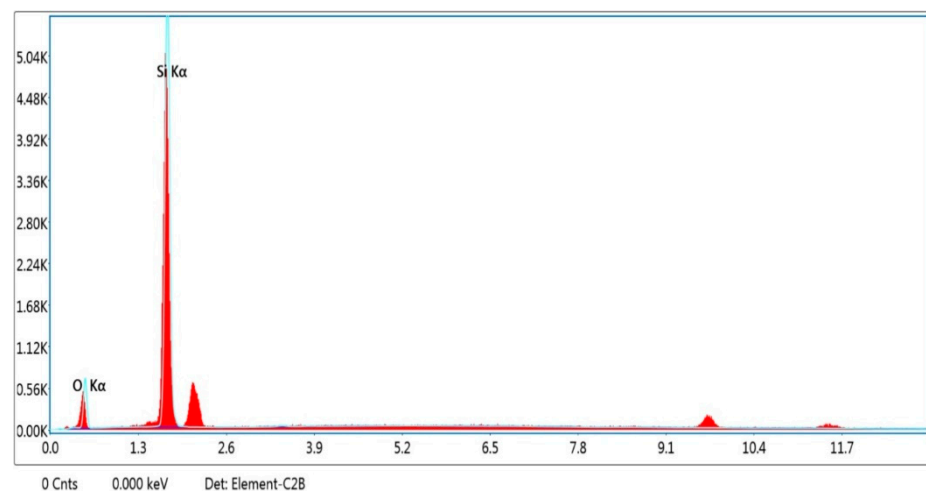


Figure 3. XRD graph of the nano-silica used in this research.

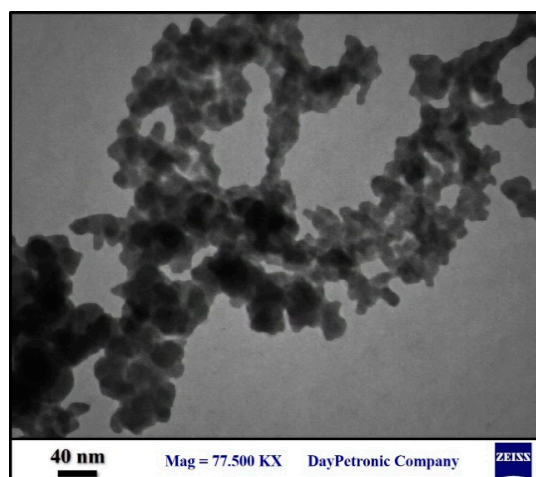


Figure 4. TEM image of the nano-silica used in this research. Source: DayPetronic Company (Tehran, Iran).

Hooked end steel fiber with a length of 50 mm was used in the SFRLWC samples. The characteristics of the steel fibers and a view of them are presented in Table 2 and Figure 5, respectively.

Table 2. Mechanical and physical properties of the steel fibers used in this research.

Shape	Cross-Sectional shape	Length (mm)	Diameter (mm)	L/D	Tensile Strength (MPa)	Density (Kg/m ³)
Hooked	Circular	50	0.8	62.5	1200	7850

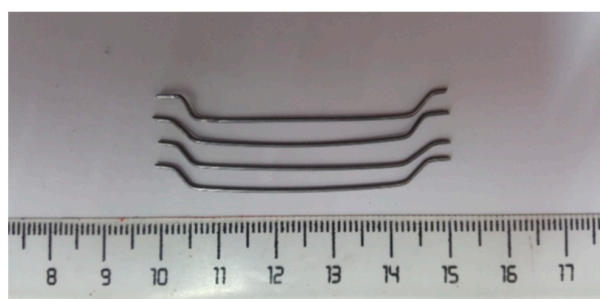


Figure 5. Steel fiber with hooked end.

The concrete mix design was determined according to ACI 211.2 [1]. The maximum dimensions of the aggregate and the slump were considered to be 12.5 mm and 70–80 mm, respectively, when determining the mixture design. The LWC mix design used in all samples is presented in Table 3.

Table 3. The LWC mix design per cubic meter used in all samples in this research.

Concrete Type	Cement (kg/m ³)	Coarse Aggregate (kg/m ³)	Fine Aggregate (kg/m ³)	W/C %	Super Plasticizer	Target f'_c (MPa)	Specific Weight (kg/m ³)
LWC	450	350	850	0.38	2%	32	1910

2.2. Preparation of Test Samples

To achieve a uniformly fresh LWC for all samples, the coarse and fine aggregate were dried at a room temperature of 25 °C for 24 h. Then, aggregates and cement were mixed in the mixture for about 2 min. If nano-silica is to be added to the mixture, it is mixed by

cement first before being mixed by aggregate. Water and superplasticizer were then mixed and added to the mixture for the next 5 min in two parts. If steel fibers are to be added to the mixture, then they are integrated gradually. After the final mixing for another 5 min to achieve a homogeneous mixture, steel molds were filled with the fresh concrete and vibrated for 30 s in two layers. Samples were cylindrical 100×200 mm specimens and were employed for axial compressive strength, tensile splitting strength and axial stress–strain curves tests.

The samples prepared and tested in this research belonged to one of the four groups. For the first group, a control specimen was prepared without fibers and nano-silica. For the second group, samples with steel fibers of 1%, 1.5%, and 2% volumetric fraction of LWC were added to the mixture. For the third group, nano-silica of 1%, 3%, and 5% of the cement's weight were added to the LWC. Finally, the samples in the fourth group were prepared with 1% fibers and 3% nano-silica. The details of the samples prepared for the tests are presented in Table 4. A total number of about 280 samples were prepared for tests. Samples were taken out of the mold and treated by being covered with a wet cloth and nylon for the following 28 day (see Figure 6). After that, they were stored at a room temperature of 25 °C for another 62 days to be prepared for their subjection to high temperatures.

Table 4. Details of the samples.

Design Group	Specimen	Steel Fibers (%) (Volumetric Fraction)	Nano-Silica (%) (of Cement Weight)
First group (LWC)	LWC	-	-
	LWF1	1	-
Second group (SFRLWC)	LWF1.5	1.5	-
	LWF2	2	-
	LWN1	-	1
Third group (NSLWC)	LWN3	-	3
	LWN5	-	5
Fourth group (ComboSFNSLWC)	LWN3F1	1	3



Figure 6. The samples covered with wet cloth and nylon.

2.3. Heat Treatment

Ninety-day-aged samples were placed in a furnace with a chamber size of 1.2 m \times 0.8 m \times 2.4 m for 24 h at 110 °C in order to dry. Then, thermal conditions of 200 °C, 400 °C, and 600 °C were applied to them. During the preheating phase, the temperature was increased at a rate of 5 degrees per minute; however, a slower increase in temperatures was applied during the main cycles. The samples were then left at the maximum temperature for another hour before the furnace was turned off and the process of natural cooling begun. A view of the samples prepared in the furnace is depicted in Figure 7. To record the temperature increment, two thermocouple sensors were placed in the furnace. One to record the ambient temperature and the second one, placed in the

middle of a $100 \times 100 \times 100$ mm concrete cube, to record the temperature of the concrete's core. The temperature–time curves for the main heating cycles of the furnace are shown in Figure 8. As can be noticed, the concrete samples' core temperatures are less than the ambient temperature. After reaching room temperature, all of the test samples were stored in the laboratory for an additional 14 days before the tests.



Figure 7. The samples prepared inside the furnace.

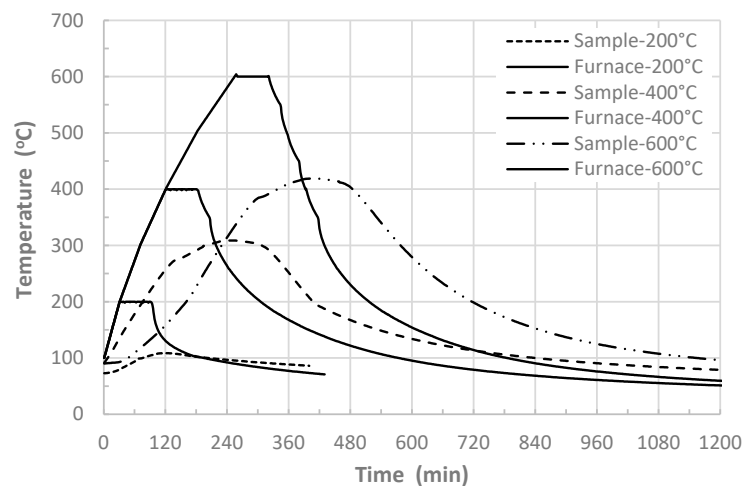


Figure 8. Temperature–time curve for the furnace and the samples' cores.

3. Results and Discussion

The samples that experienced temperatures of 200 °C, 400 °C and 600 °C were subjected to the compressive and tensile tests, and their elastic modulus and stress–strain curves were determined—as described in the following—and compared with those obtained from the control samples.

In a compression test, samples were subjected to an axial loading rate of 1.25 mm/min. The loading process was displacement-controlled and continued until the samples were destroyed (as shown in Figure 9a). The Brazilian tensile strength (BTS) test was conducted to determine the tensile strength of the samples. The compressive force applied along the top and bottom side of the cylinder caused a tensile crack to open up in a direction perpendicular to the direction of the compressive force (as shown in Figure 9b). The tensile force could then be calculated using Equation (1).

$$f_t = \frac{2P}{\pi LD} \quad (1)$$

where P is the maximum load in N, and L and D are the samples length and diameter in mm, respectively.

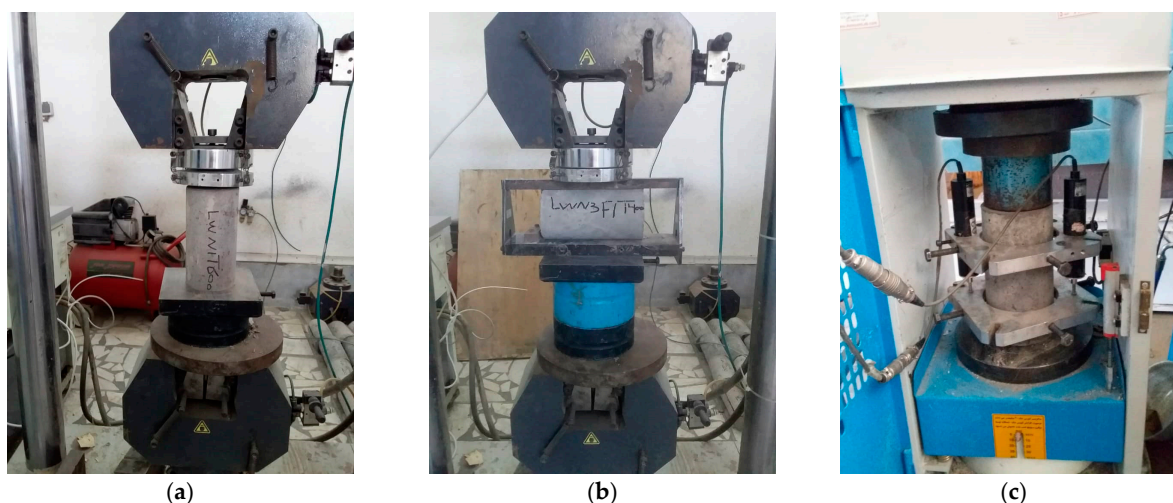


Figure 9. Test devices for (a) compressive strength, (b) tensile strength, and (c) stress–strain curve.

The stress–strain curves were obtained from a compressive test while a ring was connected to the cylindrical samples with two LVDTs to record the half middle deflection of samples. This was undertaken in order to calculate the strain correctly based on ASTM C469 [31], as shown in Figure 9c. These LVDTs were installed symmetrically on the samples and so the average of the measured values was used to determine the axial strain. These measured strains and applied loads were then used to derive the stress–strain curves of the concrete samples, which were also utilized to determine the elastic modulus. The axial load and the axial deformation were recorded using a datalogger. The peak stress and strain thus derived from the reported curve and the elastic modulus were calculated using Equation (2) [31].

$$E = (s_2 - s_1) / (\varepsilon_2 - 0.000050) \quad (2)$$

where E is the modulus of elasticity in MPa, S_2 is the stress corresponding to 40% of the ultimate load, S_1 is the stress corresponding to a longitudinal strain of 50 millionths in MPa, and ε_2 is the longitudinal strain produced by stress S_2 .

3.1. Compressive Strength

The compressive strengths of the tested samples obtained from the tests are shown in Table 5. The results indicate that the addition of different fractions of steel fibers to the LWC increased the compressive strength of the control samples at room temperature. The highest increase in compressive strength corresponded to the samples with 1% steel fiber; however, the effect of steel fiber on the compressive strength is negligible. Adding higher percentages of steel fiber reduced the compressive strength. This is due to the fact that the main role of the fibers is to prevent crack growth and that using more fibers can lead to necking, which undermines crack repair and results in lower compressive strength.

Table 5. Compressive strength of the samples at various temperatures (MPa).

Specimen	25 °C	200 °C	400 °C	600 °C
LWC	33.1	30.0	22.8	17.6
LWF1	34.9	33.0	28.5	22.0
LWF1.5	34.1	32.4	28.0	22.7
LWF2	33.8	32.2	27.8	22.5
LWN1	36.6	34.3	32.4	24.4
LWN3	43.8	42.2	40.1	32.4
LWN5	41.2	39.1	34.7	28.3
LWN3F1	46.0	44.4	43.1	37.9

The addition of different percentages of nano-silica to the LWC samples at room temperature improved the hydration and microstructure of the concrete, thus increasing the compressive strength in all of the LWC samples as expected. However, high percentages of nano-silica (i.e., 5%) produced lower compressive strengths compared with lower percentages (i.e., 3%) as they increased the volume of different hydration products at the aggregate–cement paste interface (i.e., the ITZ). The best specimen in the case of compressive strength contained a combination of 1% fiber and 3% nano-silica and resulted in a 39% increase in compressive strength, mostly because of the nano-silica, compared with the LWC (control sample).

The trend of the compressive strength for the samples at 200 °C, 400 °C, and 600 °C were individually similar to those for the samples at 25 °C, with the difference being a less strong reduction in compressive strength in the samples with a higher fiber percentage as shown in Figure 10. In general, decrements in the compressive strength were observed while elevating the temperature when compared with the control samples. Figure 10a compares the compressive strengths in different samples and at different temperatures. In addition, Figure 10b shows the residual compressive strength of each sample in comparison with the control sample. As the results indicate, the deterioration in LWC when subjected to a high temperature is dramatic. Adding steel fiber or nano-silica substantially reduces the deterioration of compressive strength and the residual capacity is much closer to the control sample. The compressive strengths of the samples decreased in a nonlinear manner while subjected to elevated temperature.

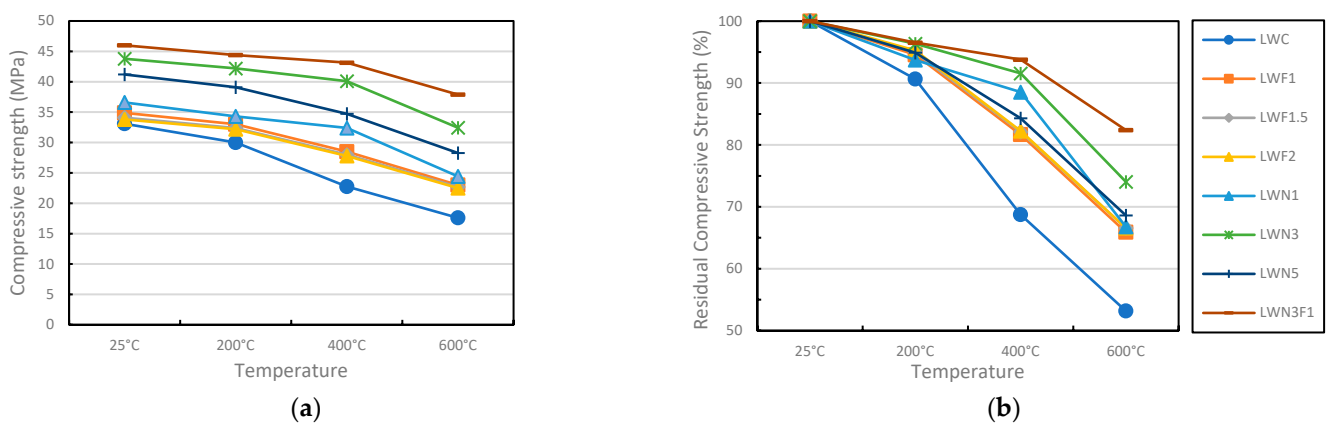


Figure 10. Results for different temperatures. (a) Compressive strength and (b) residual compressive strength.

As shown in Figure 11, the deterioration of compressive strength in all samples were observable when they were subjected to elevated temperatures. However, the temperature rise had a smaller effect on the samples with fibers and nano-silica. This was due to the smaller decrease in the compressive strength of the fibers and nano-silica at 200 °C.

As can be seen in Figure 12, The color changes of all kinds of concrete were observed in all heat degrees. Indeed, the concrete color was light grey at room temperature while the surface color became pink grey at 600 °C and the color of the samples at 200 °C and 400 °C was something between. Moreover, the mechanism of fracture changes when adding steel fiber or nano-silica to the LWC. Delays to the concrete spalling and crack propagation were observable in the samples with additives.

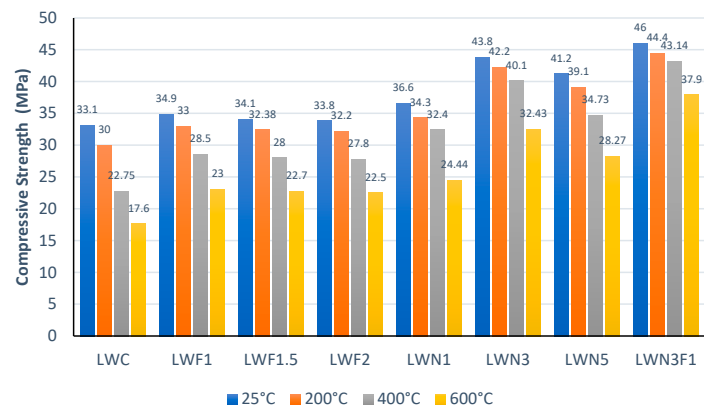


Figure 11. Comparison of the compressive test results of different samples at different temperatures.

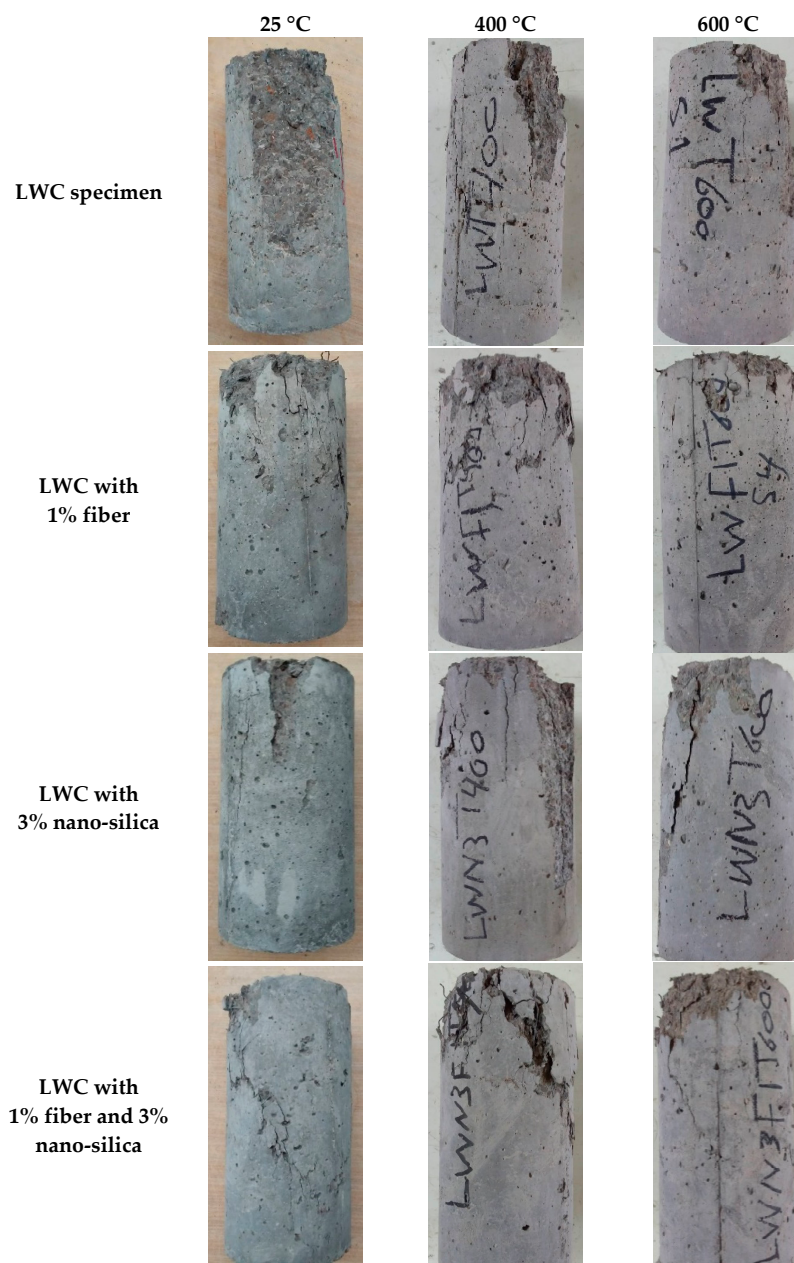


Figure 12. Images showing the compressive test results of different samples at different temperatures.

3.2. Tensile Strength

The tensile strengths of the tested samples obtained from The BTS and calculated by Equation (1) are shown in Table 6. Based on the results, with a 2% increase in the percentage of steel fibers, the tensile strength of control samples at room temperature increased by about 100% due to the capacity that steel fibers apply to the LWC. However, the increase in tensile strength became slightly smaller as the percentage of steel fibers increased. Specifically, the addition of 1%, 1.5%, and 2% steel fibers to the samples resulted in a 50%, 76%, and 96% increase in tensile strength, respectively. Similar to the compressive strength of LWC with nano-silica, the best percentage of nano-silica was observed to be at 3%. This is because there is an excessive unused increase in hydration products at higher percentages of nano-silica. The addition of nano-silica to the samples with 1% steel fibers increased the tensile strength compared with the samples with only steel fibers or nano-silica on their own. However, the strength of these samples was smaller than those with 2% fiber (and without nano-silica).

Table 6. Tensile strength of the samples at various temperatures (MPa).

Specimen	25 °C	200 °C	400 °C	600 °C
LWC	3.0	2.6	2.3	1.4
LWF1	4.5	4.2	3.4	3.2
LWF1.5	5.3	5.5	4.6	3.8
LWF2	5.9	5.7	5.4	4.5
LWN1	3.4	3.2	2.7	2.4
LWN3	4.0	3.8	3.4	2.7
LWN5	3.8	3.6	3.2	2.4
LWN3F1	5.1	4.9	4.6	4.0

In the samples at 200 °C, 400 °C, and 600 °C, the tensile strength exhibited a trend similar to that of the samples at 25 °C. The tensile strength of the samples increased with a rise in the percentage of steel fibers due to the increase in the tensile capacity and ductility of the samples. However, in the samples with nano-silica, high percentages of nano-silica decreased the tensile strength because of the production of new unused hydration products. Figure 13 compares the tensile strength and residual tensile strength in different samples and at different temperatures. Results clearly indicate the dramatic loss of capacity in LWC when subjected to elevated temperature. Additives can enhance this deterioration. The effectiveness of additives to the tensile strength and residual capacity of samples are dedicated to both steel fibers and nano-silica.

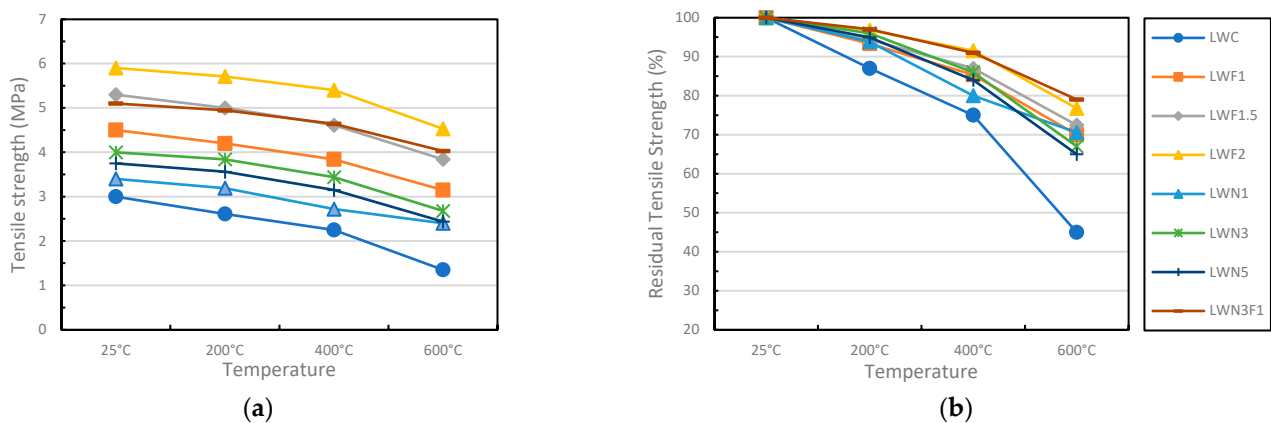


Figure 13. Results for different temperatures. (a) Tensile strength and (b) residual tensile strength.

As shown in Figure 14, a deterioration of tensile strength can be observed in all samples when they are subjected to elevated temperature. However, this decrease was in a

similar to the trends of samples with fibers and nano-silica. Hence, the temperature rise had a smaller effect on these samples.

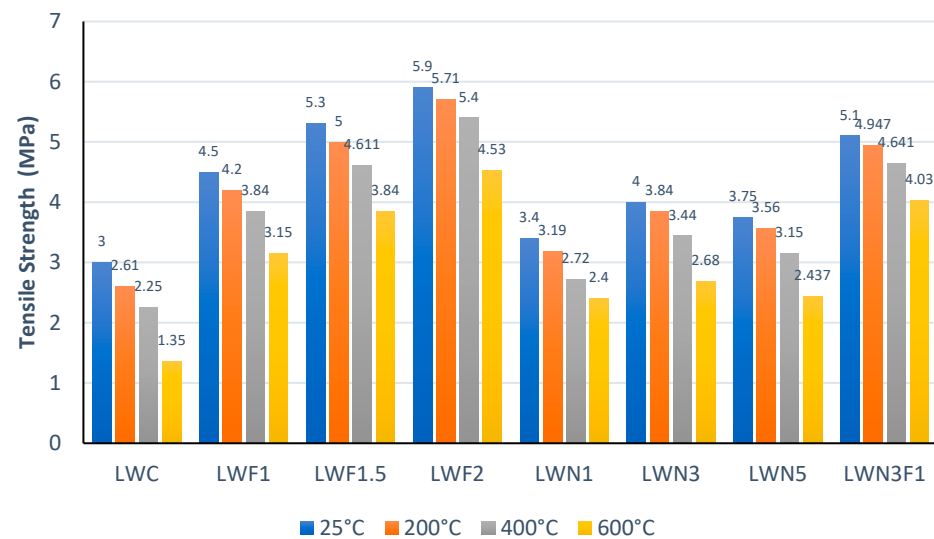


Figure 14. Comparison of the tensile test results of different samples at different temperatures.

The tensile strengths of the samples decreased in a nonlinear manner while subjected to elevated temperature. Much greater strength loss was observed for the specimen without fibers and nano-silica (i.e., the control specimen). Strength reduction was smaller in samples with additives due to the contribution of nano-silica and steel fiber to the strength of the samples at high temperatures. For the samples at 600 °C, the tensile strengths exhibited a trend similar to those of the previous samples. It is notable to point out the reduction of both compressive and tensile strengths with a rise in temperature, which is due to the reduction of the relevant properties of the concrete at high temperatures, leading to a drop in the strengths of the samples. The tensile fracture of samples with and without fibers are displayed in Figure 15.



(a)



(b)

Figure 15. Tensile fracture of the specimen with (a) 1% fiber and 3% nano-silica and (b) LWC at room temperature.

3.3. Modulus of Elasticity

The results corresponding to the modulus of elasticity of the various samples under study were calculated based on Equation (2) and are presented in Table 7.

Table 7. Modulus of elasticity of different samples at different temperatures.

Specimen	25 °C	200 °C	400 °C	600 °C
LWC	14.7	10.0	6.1	3.5
LWF1	15.1	11.1	7.1	4.0
LWN3	15.5	12.0	8.9	5.4
LWN3F1	16.3	12.7	9.1	5.7

As seen in Table 7 and Figure 16, the modulus of elasticity was smaller than normal concrete and decreased in all the samples with an increase in temperature. This is because of the decreasing effect of temperature on the properties of different components in the LWC. However, adding steel fiber can harden the samples and hence a steeper initial slope is observed. The bridging effect of steel fiber inside samples was clearly another primary reason for the greater modulus of elasticity reported previously [32]. Furthermore, the specimen with both fibers and nano-silica possessed the highest modulus of elasticity, while LWC possessed the smallest modulus of elasticity among all of the samples. Moreover, between fibers and nano-silica, the samples with nano-silica exhibited a higher modulus of elasticity. This is due to the enhancement of hydration and concrete microstructure by nano-silica and the lack of micro-crack development at the early stage of axial loading, something which steel fiber could have an effect on.

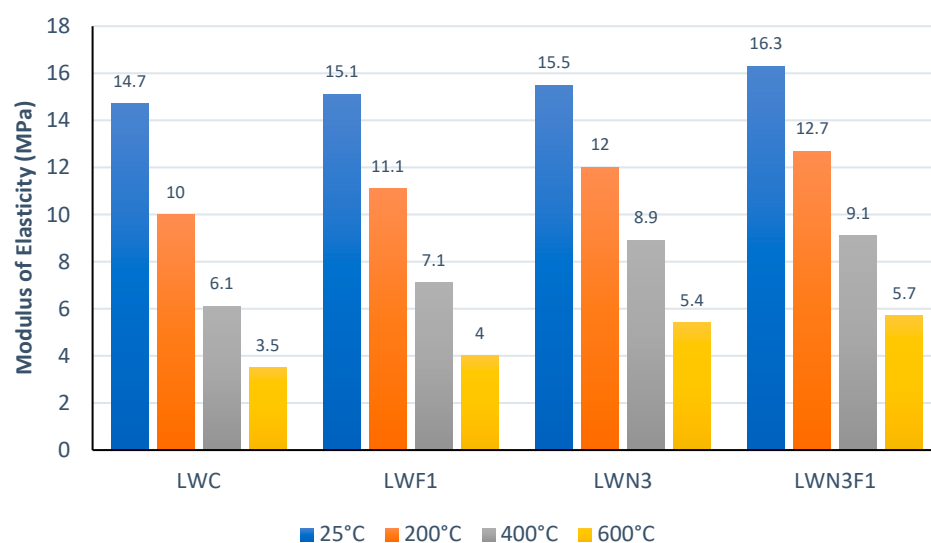


Figure 16. Comparison of the modulus of elasticity results of different samples at different temperatures.

3.4. Stress–Strain Curves

The stress–strain curves at temperatures of 25 °C, 200 °C, 400 °C, and 600 °C for the control samples (LWC), the samples with 1% fibers (LWF1), the samples with 3% nano-silica (LWN3), and the samples with 1% fiber and 3% nano-silica (LWF1N3) are displayed in Figure 17. Due to some limitations, the results are shown as far as the maximum stress.

As seen in Figure 17a, the maximum stress, the strain, and the modulus of elasticity all increased with an increase in the steel fiber percentage. Additionally, substituting the steel fibers with nano-silica further increased the values by improving the concrete microstructure and the hydration process and increasing the ductility. The simultaneous addition of nano-silica and steel fibers positively affected the stress–strain curve and increased both the stress and the strain capacities of LWC. The best condition was obtained

with 1% fibers and 3% nano-silica. Such a slight increase in compressive stress while using steel fibers and the improvement of the post-peak compressive behavior has also been observed in other research [33,34].

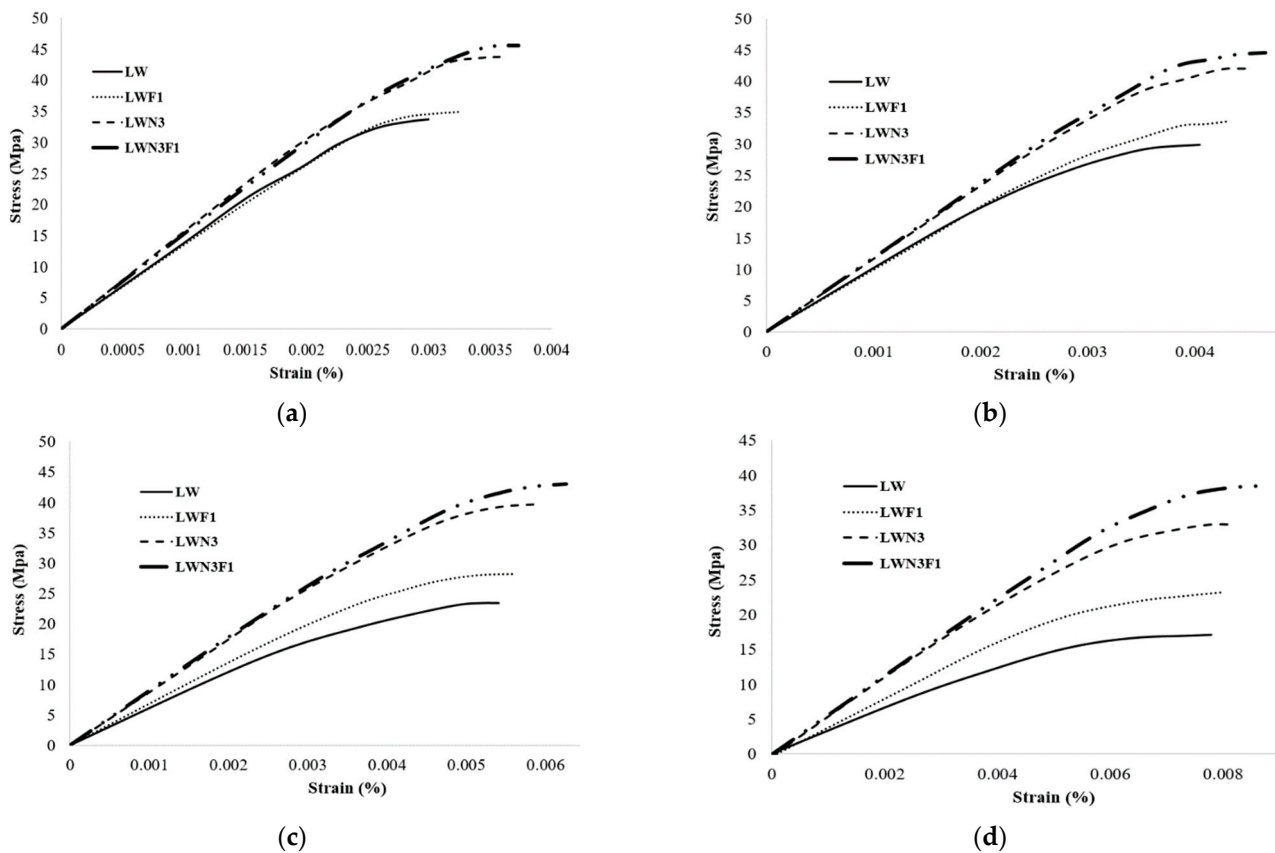


Figure 17. Stress–strain curves of different samples at (a) 25 °C, (b) 200 °C, (c) 400 °C, and (d) 600 °C.

Consequently, the stress–strain curves of all samples gradually flattened. For 600 °C, the strength and stiffness for the LWC samples showed much greater losses than other samples, and the areas under the stress–strain curves also decreased more sharply than those of SFRLWC and NSLWC.

Additionally, as indicated in Figure 17, the peak strain increased with a rise in temperature due to the softening of the concrete components and the difference in the thermal properties of the aggregate and the cement paste. This can also be attributed to the considerable decomposition of the cement paste, which increases porosity in the concrete and creates small cracks in the transition zone [6].

4. Conclusions

This research conducted a study of the post-fire mechanical degradation of lightweight concrete (LWC). Moreover, the addition of steel fiber and nano-silica have been investigated in terms of their abilities to reduce the mechanical degradation of LWC subjected to high temperatures, and hence to obtain a sustainable material. For this purpose, different samples were casted in four mixture designs: the LWC samples; samples with steel fibers; samples with nano-silica; and samples with a combination of steel fibers and nano-silica. All samples were subjected to temperatures of 200, 400 and 600 degrees Celsius and were compared with the control samples. Subsequently, tests were performed to determine the compressive and tensile strengths as well as the modulus of elasticity and stress–strain curves of the LWC samples with or without steel fibers and nano-silica. The research results can be summarized as follows:

- 1 As the temperature was elevated, both the compressive and tensile strengths decreased in a nonlinear manner for all of the samples. However, a much greater strength loss was observed for LWC, which is not preferable in the construction industry despite the advantages that smaller self-weight can gift to structures. The strength reduction was slower in SFRLWC and NSLWC due to the contribution of nano-silica and steel fiber to the strength of the samples at high temperatures.
- 2 Results indicate that additives such as steel fiber and nano-silica can enhance the strength of LWC while it is subjected to higher temperatures. The effectiveness of this improved performance in the tensile capacity can be attributed to the steel fibers because of their ability to bridge between cracks and reduce crack propagation. Meanwhile, nano-silica affects the compressive strength and the modulus of elasticity considerably better, due to its effect on the hydration process and the concrete microstructure. When using both steel fiber and nano-silica, results indicate that all the mechanical properties studied here were improved significantly.
- 3 In the samples with fibers or nano-silica, cracking, crack propagation and local damage were smaller than in the other samples. At the same time, crack dispersion and uniformity improved. The steel fibers successfully prevented crack growth in the concrete samples subjected to high heat and performed better than nano-silica in this regard.
- 4 According to the stress–strain curves obtained for the samples, the peak strain increased with an increase in the steel fibers. Moreover, the replacement of steel fibers with nano-silica further increased peak stress and strain. The best condition corresponded to 1% fibers and 3% nano-silica. In all the samples, the rise in temperature flattened the stress–strain curve. It is assumed that, since the modulus of elasticity was calculated at one-fourth of the peak stress, the micro-cracks were not yet developed and, consequently, the steel fiber effect was relatively small. Therefore, the elevated temperature has a significant effect on SFLWC, even in larger amount of steel fiber volume fraction.

Author Contributions: Investigation, A.F.M. and S.K.H.; supervision, S.K.H. and H.T.; validation, A.F.M., S.K.H. and H.T.; writing—original draft, A.F.M.; writing—review and editing, S.K.H. All authors have read and agreed to the published version of the manuscript.

Funding: This research was funded by Babol Noshirvani university of technology, grant number BNUT/395803/401.

Institutional Review Board Statement: Not applicable.

Informed Consent Statement: Not applicable.

Data Availability Statement: Not applicable.

Acknowledgments: The authors would like to express their appreciation for the LECA material provided by Leca Provider Company [28].

Conflicts of Interest: The authors declare no conflict of interest.

References

1. ACI213R-14: *Guide for Structural Lightweight-Aggregate Concrete*; ACI: Miami, FL, USA, 2014.
2. Zhou, J.; Wang, L. Repair of Fire-Damaged Reinforced Concrete Members with Axial Load: A Review. *Sustainability* **2019**, *11*, 963. [[CrossRef](#)]
3. Szép, J.; Habashneh, M.; Lógó, J.; Rad, M.M. Reliability Assessment of Reinforced Concrete Beams under Elevated Temperatures: A Probabilistic Approach Using Finite Element and Physical Models. *Sustainability* **2023**, *15*, 6077. [[CrossRef](#)]
4. Ganesan, H.; Sachdeva, A.; Petrounias, P.; Lampropoulou, P.; Sharma, P.K.; Kumar, A. Impact of Fine Slag Aggregates on the Final Durability of Coal Bottom Ash to Produce Sustainable Concrete. *Sustainability* **2023**, *15*, 6076. [[CrossRef](#)]
5. Bideci, S.; Yılmaz, H.; Gencil, O.; Bideci, A.; Çomak, B.; Nodehi, M.; Ozbakkaloglu, T. Fiber-Reinforced Lightweight Calcium Aluminate Cement-Based Concrete: Effect of Exposure to Elevated Temperatures. *Sustainability* **2023**, *15*, 4722. [[CrossRef](#)]
6. Dabbaghi, F.; Dehestani, M.; Yousefpour, H.; Rasekh, H.; Navaratnam, S. Residual compressive stress–strain relationship of lightweight aggregate concrete after exposure to elevated temperatures. *Constr. Build. Mater.* **2021**, *298*, 123890. [[CrossRef](#)]

7. Tanyildizi, H.; Coşkun, A. Performance of lightweight concrete with silica fume after high temperature. *Constr. Build. Mater.* **2008**, *22*, 2124–2129. [[CrossRef](#)]
8. Wang, H.; Wei, M.; Wu, Y.; Huang, J.; Chen, H.; Cheng, B. Mechanical Behavior of Steel Fiber-Reinforced Lightweight Concrete Exposed to High Temperatures. *Appl. Sci.* **2020**, *11*, 116. [[CrossRef](#)]
9. Ismail, K.M.; Fathi, M.S.; Manaf, N. *Study of Lightweight Concrete Behaviour*; Universiti Teknologi Malaysia: Johor Bahru, Malaysia, 2004.
10. Van Chanh, N. Steel Fiber Reinforced Concrete. In Faculty of Civil Engineering Ho Chi Minh City University of Technology; Seminar Materi-al. 2004. Available online: [https://www.jsce.or.jp/committee/concrete/e/newsletter/newsletter05/8-Vietnam%20Joint%20Seminar\(CHANH\).pdf](https://www.jsce.or.jp/committee/concrete/e/newsletter/newsletter05/8-Vietnam%20Joint%20Seminar(CHANH).pdf) (accessed on 29 March 2022).
11. Song, P.S.; Hwang, S. Mechanical properties of high-strength steel fiber-reinforced concrete. *Constr. Build. Mater.* **2004**, *18*, 669–673. [[CrossRef](#)]
12. Dvorkin, L.; Zhitkovsky, V.; Ribakov, Y. A method for optimal design of steel fiber reinforced concrete composition. *Mater. Des.* **2011**, *32*, 3254–3262. [[CrossRef](#)]
13. Abbass, W.; Khan, M.I.; Mourad, S. Evaluation of mechanical properties of steel fiber reinforced concrete with different strengths of concrete. *Constr. Build. Mater.* **2018**, *168*, 556–569. [[CrossRef](#)]
14. Guler, S.; Akbulut, Z.F. Residual strength and toughness properties of 3D, 4D and 5D steel fiber-reinforced concrete exposed to high temperatures. *Constr. Build. Mater.* **2022**, *327*, 126945. [[CrossRef](#)]
15. Wang, H.; Wang, L. Experimental study on static and dynamic mechanical properties of steel fiber reinforced lightweight aggregate concrete. *Constr. Build. Mater.* **2013**, *38*, 1146–1151. [[CrossRef](#)]
16. Grabois, T.M.; Cordeiro, G.C.; Filho, R.D.T. Fresh and hardened-state properties of self-compacting lightweight concrete reinforced with steel fibers. *Constr. Build. Mater.* **2016**, *104*, 284–292. [[CrossRef](#)]
17. Balendran, R.; Zhou, F.; Nadeem, A.; Leung, A. Influence of steel fibres on strength and ductility of normal and lightweight high strength concrete. *Build. Environ.* **2002**, *37*, 1361–1367. [[CrossRef](#)]
18. Almasabha, G.; Murad, Y.; Alghossoon, A.; Saleh, E.; Tarawneh, A. Sustainability of Using Steel Fibers in Reinforced Concrete Deep Beams without Stirrups. *Sustainability* **2023**, *15*, 4721. [[CrossRef](#)]
19. Huang, R.; Li, S.; Meng, L.; Jiang, D.; Li, P. Coupled Effect of Temperature and Strain Rate on Mechanical Properties of Steel Fiber-Reinforced Concrete. *Int. J. Concr. Struct. Mater.* **2020**, *14*, 48. [[CrossRef](#)]
20. Kalpana, M.; Tayu, A. Light weight steel fibre reinforced concrete: A review. *Mater. Today Proc.* **2020**, *22*, 884–886. [[CrossRef](#)]
21. Balapour, M.; Joshaghani, A.; Althoey, F. Nano-SiO₂ contribution to mechanical, durability, fresh and microstructural characteristics of concrete: A review. *Constr. Build. Mater.* **2018**, *181*, 27–41. [[CrossRef](#)]
22. Nazari, A.; Riahi, S. Microstructural, thermal, physical and mechanical behavior of the self compacting concrete containing SiO₂ nanoparticles. *Mater. Sci. Eng. A* **2010**, *527*, 7663–7672. [[CrossRef](#)]
23. Beigi, M.H.; Berenjian, J.; Omran, O.L.; Nik, A.S.; Nikbin, I.M. An experimental survey on combined effects of fibers and nanosilica on the mechanical, rheological, and durability properties of self-compacting concrete. *Mater. Des.* **2013**, *50*, 1019–1029. [[CrossRef](#)]
24. Yu, R.; Spiesz, P.; Brouwers, H.J.H. Effect of nano-silica on the hydration and microstructure development of Ultra-High Performance Concrete (UHPC) with a low binder amount. *Constr. Build. Mater.* **2014**, *65*, 140–150. [[CrossRef](#)]
25. Mohamed, A.M. Influence of nano materials on flexural behavior and compressive strength of concrete. *HBRC J.* **2016**, *12*, 212–225. [[CrossRef](#)]
26. Wang, X.; Huang, Y.; Wu, G.; Fang, C.; Li, D.; Han, N.; Xing, F. Effect of nano-SiO₂ on strength, shrinkage and cracking sensitivity of lightweight aggregate concrete. *Constr. Build. Mater.* **2018**, *175*, 115–125. [[CrossRef](#)]
27. Tobbala, D.E.; Rashed, A.S.; Tayeh, B.A.; Ahmed, T.I. Performance and microstructure analysis of high-strength concrete incorporated with nanoparticles subjected to high temperatures and actual fires. *Arch. Civ. Mech. Eng.* **2022**, *22*, 1–15. [[CrossRef](#)]
28. Leca Provider Company. Available online: <https://leca.asia/> (accessed on 29 March 2022).
29. *ASTMC330/C330M*; Standard Specification for Lightweight Aggregates for Structural Concrete. ASTM International: West Conshohocken, PA, USA, 2014.
30. *ASTMC33*; Standard Specification for Concrete Aggregates. ASTM International: West Conshohocken, PA, USA, 2018.
31. *ASTMC469*; Standard Test Method for Static Modulus of Elasticity and Poisson’s Ratio of Concrete in Compression. ASTM International: West Conshohocken, PA, USA, 2014.
32. Zeng, J.-J.; Wang, J.-S.; Ouyang, Y.; Zhuge, Y.; Liao, J.; Long, Y.-L.; Zhou, J.-K. Tri-axial compressive behavior of expansive concrete and steel fiber-reinforced expansive concrete. *J. Build. Eng.* **2023**, *68*, 106026. [[CrossRef](#)]
33. Voutetaki, M.E.; Naoum, M.C.; Papadopoulos, N.A.; Chalioris, C.E. Cracking Diagnosis in Fiber-Reinforced Concrete with Synthetic Fibers Using Piezoelectric Transducers. *Fibers* **2022**, *10*, 5. [[CrossRef](#)]
34. Smarzewski, P. Study of Toughness and Macro/Micro-Crack Development of Fibre-Reinforced Ultra-High Performance Concrete After Exposure to Elevated Temperature. *Materials* **2019**, *12*, 1210. [[CrossRef](#)]

Disclaimer/Publisher’s Note: The statements, opinions and data contained in all publications are solely those of the individual author(s) and contributor(s) and not of MDPI and/or the editor(s). MDPI and/or the editor(s) disclaim responsibility for any injury to people or property resulting from any ideas, methods, instructions or products referred to in the content.